PHYSICAL REVIEW A VOLUME 57, NUMBER 6 JUNE 1998

Absolute rates for radiative and nonradiative collisional deexcitation of metastable $He^+(2s)$ ions

H. T. Schmidt, S. H. Schwartz, and H. Cederquist
Department of Physics, Atomic Physics, Stockholm University, S-104 05 Stockholm, Sweden

L. Liljeby
Manne Siegbahn Laboratory, Stockholm University, S-104 05 Stockholm, Sweden

J. C. Levin and I. A. Sellin
Department of Physics and Astronomy, University of Tennessee, Knoxville, Tennessee 37996-1200

(Received 6 March 1998)

A method devised to measure separate absolute rates for deexcitation of metastable hydrogenic atoms and ions via radiative and nonradiative processes is applied in a pilot study of 6.6-keV $He^+(2s)$-Ar $\rightarrow He^+(1s)$-... collisions. An absolute total deexcitation cross section $\sigma_{de}^{tot}=(7.6\pm1.2)\times10^{-16}$ cm^2 was measured by attenuation. The cross section for nonradiative deexcitation was then measured independently. A radiative branching ratio $R_{BR}=(70\pm8)\%$ was determined, without requiring absolute photon detection calibrations. The measured radiative deexcitation cross section agrees with the result of a semiclassical calculation when competing capture and ionization processes are taken into account. [S1050-2947(98)50406-4]

PACS number(s): 34.50.Fa, 32.10.Dk, 52.20.Hv

When a slow excited atom collides with a ground-state atom or molecule with an ionization potential lower than the excitation energy, the projectile may deexcite via target ionization [1,2]. This process, which may proceed through different mechanisms, was first identified by Penning [1]. The literature concerning Penning ionization by metastable atoms is vast, and has been expertly reviewed recently [2], mainly for collisions occurring near thermal energies. By contrast, the literature concerning Penning ionization by metastable ions is very sparse.

Penning ionization (PI) by ions seems to have been first taken up theoretically by Lamb in connection with refining pioneering rf resonance measurements by Lamb, Skinner, Novick, and Lipworth [3] of radiative level shifts in $He^+(2s)$ ions created by electron impact. In this context, depletion of $He^+(2s)$ population due to near-thermal $He^+(2s)$-$He(1s^2)$ collisions was deemed important to consider. The calculated [3] (not measured) values of the radiative (R) and nonradiative (NR) deexcitation cross sections σ_{de}^{R} and σ_{de}^{NR} were 3.03×10^{-15} cm^2 and 1.40×10^{-15} cm^2, respectively, at prevailing ion speeds $v\sim1.05\times10^5$ cm/s (kinetic energy, 23 meV). The principal R (1) and NR (2) deexcitation branches identified at these thermal velocities were the following [3]. The ion charge induces a dipole moment in a neighboring atom. The ion and the atom are in relative motion, so that the dipole field sweeps over the ion and induces transitions to the nearly degenerate $2p$ states, whence there is Ly-α decay after the collision:

$$He^+(2s)+X\rightarrow He^+(2p)+X\rightarrow He^+(1s)+X+h\nu. \quad (1)$$

The lifetime of the $2p$ state is 100 ps, which is long compared to the collision time, even at these thermal energies. Autoionization of the quasimolecular collision complex results in Penning ionization

$$He^+(2s)+X\rightarrow He^+(1s)+X^+ +e^-. \quad (2)$$

Currently, there is a strong fusion physics interest in the absolute cross sections for NR and R deexcitation of $He^+(2s)$ at higher energies—up to a few hundred eV [4]. These metastable ions (formed by resonant electron capture in He^{2+}-H collisions) are abundant in fusion plasmas and their interactions with major fusion constituents are significant for helium transport in tokamak plasma edge regions. Further, the present $He^+(2s)$-Ar collisions are of specific interest since N, N_2, Ne, Ar, and Kr are being considered for injection at the plasma periphery to enhance plasma edge radiation cooling [4].

We know of only four experiments concerned with collisional deexcitation of metastable ions, including ours, which we believe to be unique because it establishes *separate absolute* values for σ_{de}^{R} and σ_{de}^{NR}. In connection with a time-of-flight determination of the $He^+(2s)$ lifetime, Kocher *et al.* [5], measured the total collisional deexcitation cross section, σ_{de}^{tot}, for 15-eV $He^+(2s)$ in He and N_2. Soon thereafter Prior and Wang [6] determined corresponding rate constants for $He^+(2s)$ ions held in a trap, colliding at an average kinetic energy of 230 meV with noble gases and with various nonpolar and polar molecules. A few years later Shah and Gilbody [7] determined σ_{de}^{tot}'s for $^3He^+(2s)$ ions, colliding at 5–20 keV/u with various targets.

In this work we present results based on a technique devised to measure σ_{de}^{tot} in an attenuation measurement and σ_{de}^{NR} in a separate measurement where the recoil ion (unique to the NR deexcitation process) is detected in coincidence with the projectile ion. From these two results the absolute contribution of the radiative branch is deduced for 6.6-keV $He^+(2s)$ ions colliding with Ar. At these energies the field completely mixes the $2s$ and $2p$ levels for $\sim10^{-15}$ s. After the collision there is, as in the case of thermal collisions [3], a high probability that the ion occupies a $2p$ state and then subsequently decays to $He^+(1s)$. However, since in our work v is ~500 and in Ref. [7] ~1000 times higher than in

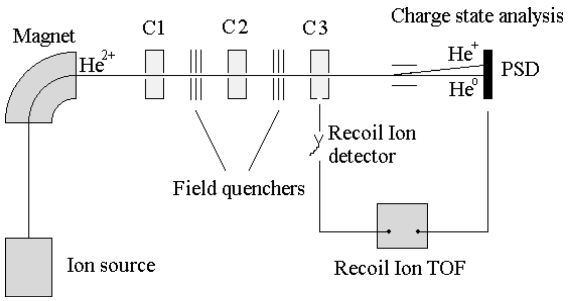

FIG. 1. Schematic of the experimental arrangement.

Refs. [3] and [6], the mechanism behind NR deexcitation differs from the one at thermal velocities. For keV collision energies NR deexcitation probably proceeds through formation of doubly excited neutral projectile states followed by autoionization at large internuclear distances. In the discussion of the present experimental result we will concentrate on a comparison between the first separate result on radiative deexcitation and a semiclassical model for collision-induced Stark mixing [6]. The agreement turns out to be excellent, provided that the influence of the main competing processes of NR deexcitation and electron capture are taken into account in the theoretical treatment.

A comprehensive account of our method, including apparatus details and various data corrections, is presented in [8]. In brief, the setup consists of three consecutive gas cells (C1,C2,C3 in Fig. 1). A He^+ beam is produced by electron capture by He^{2+} ions in Kr gas in C1, yielding a $2s$ metastable fraction F_0 of $\sim$10%. We measured a lower limit for the metastable fraction to be $F_0 \geqslant (9.1 \pm 2.6)\%$ [8]. This is consistent with $F_0 = (10 \pm 2)\%$, as found by Shah and Gilbody [7] at a slightly higher energy and we thus adopt the latter value. Originally collinear, C1, C2, and C3 are then offset and weak steering fields applied, so as to dump the remaining He^{2+} beam emerging from C1 and thread the He^+ alone through C2 and C3 to the position-sensitive detector (PSD). C3 is equipped with an ion time-of-flight (TOF) spectrometer, which is used to detect the charge states q_r of recoil ions from C3 in coincidence with scattered projectiles of specified charge $q_p = 1$ or $q_p = 0$, the only ones detected above noise on the PSD. In brief the experimental procedure is the following. First we identify a collision process in C3 that has a high cross section for $He^+(2s)$ and a low one (ideally zero) for $He^+(1s)$. The corresponding coincidence rate is thus a measure of the metastable fraction F of the beam entering C3. Now F can be altered from its entrant value F_0 at C2 by deexciting $He^+(2s)$ in a gas (here argon) in C2. The measurement of the coincidence rate at C3 as a function of the pressure in C2 yields σ_{de}^{tot} (after corrections for single-electron capture in C2). Finally σ_{de}^{NR} is obtained by recording the rate of coincidences for events in C3 where the target is ionized while the projectile charge is unaltered. In order to establish an absolute cross-section scale for σ_{de}^{tot} the pressure is measured absolutely by means of a Baratron and the effective target length is taken to be the geometrical length of C2. The absolute scale for σ_{de}^{NR} requires, in addition, knowledge of total recoil- and projectile-ion detection efficiencies (including the transmissions from the collision region to the two detectors). These are obtained by means of

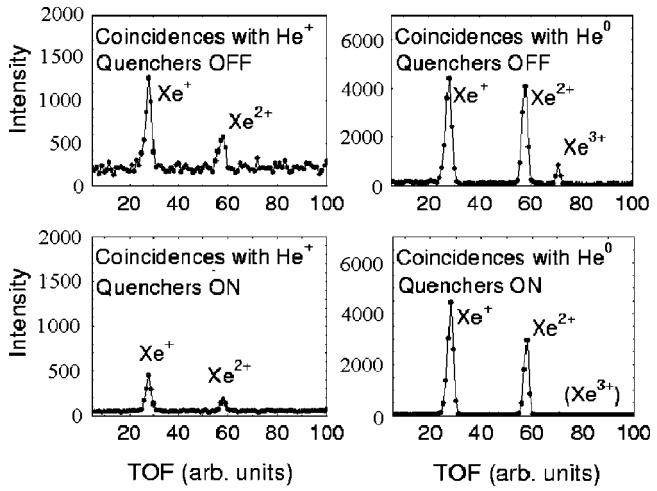

FIG. 2. TOF spectra recorded with and without electric-field quenching, with Xe in C3, in coincidence with scattered He^+ and He^0 projectiles. The spectra are recorded for the same primary ion dose and the same Xe pressure ($\sim$1 mTorr) in C3.

standard techniques routinely applied in nuclear physics, in which the coincidence rate for a process giving a unique combination of recoil and projectile charge is compared with the recoil and projectile singles rates. In effect, the products of efficiency and solid angle of both detectors are easily derived by dividing the joint coincidence rate for the two by the singles rates registered by each. Finally the absolute value of σ_{de}^{R} is determined separately through $\sigma_{de}^{R} = \sigma_{de}^{tot} - \sigma_{de}^{NR}$.

To optimize the attenuation measurements there is high payoff in using a target in C3 having a high sensitivity to $He^+(2s)$ ions. An essential tool in finding such a process is our ability to switch on and off the F_0 incident on C2, by providing a longitudinal Stark-quench field (in a weak lens configuration) between C1 and C2. Empirically we find that using Xe in C3 provides a good monitor for F after passage of C2. In Fig. 2 we show four spectra of Xe recoil ions in coincidence with He^+ and He^0—with and without electric field quenching.

There are strong influences of the $He^+(2s)$ beam component on the spectra, which change markedly when the quenching fields are applied, even though F_0 is only 10%. An appreciable amount of Xe^{3+} appears in the spectrum associated with neutralization of He^+ with the field quenchers off. This process, single electron capture accompanied by emission of two more target electrons, will in the following be denoted TDI (transfer double ionization). For pure $He^+(1s)$ beams the Xe^{3+} yield is measured to be very small. Single ionization (SI) is another process that is strongly reduced when the field quenchers are applied to give $F = 0$ (see the He^+-Xe^+ coincidences in Fig. 2). The two processes TDI and SI are used to independently gauge σ_{de}^{tot} in Ar.

As functions of the pressure of Ar in C2 we measure the effective cross section:

$$\sigma_{eff}^{i} = F\sigma_{2s}^{i} + (1-F)\sigma_{1s}^{i}, \tag{3}$$

where i = TDI or SI and σ_{1s}^{i} and σ_{2s}^{i} are the corresponding cross sections for $He^+(1s)$ and $He^+(2s)$ ions. We could thus monitor the change in F through changes of the SI and

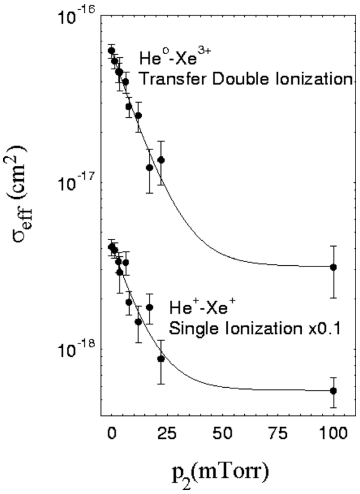

FIG. 3. $\sigma^i_{\rm eff}=F\sigma^i_{2s}+(1-F)\sigma^i_{1s}$ for i=SI and TDI as a function of Ar pressure p_2, in gas cell 2 (C2). F decreases with increasing p_2. The curves display fits to $\sigma^i_{\rm eff}$ from which $\sigma^{\rm tot}_{\rm de}$ is extracted (cf. text).

TDI signals in C3 vs Ar pressure (0–23 mTorr) in C2. Further, measuring with Stark quenching on ($F=0$) provides a simulated high (∞) pressure point (''$p2=100$ mTorr'' appearing in Fig. 3).

To extract $\sigma^{\rm tot}_{\rm de}$ we must consider how F is affected by the mixed beam collisions with Ar in C2. From Ref. [7] we can reliably estimate that for $He^+(2s)$ in Ar the cross section for electron loss is ~100 times lower than for electron capture (corroborated by never seeing He^{2+} ions at our PSD). The main processes in C2 affecting F are thus collisional deexcitation, and single-electron capture from Ar to $He^+(1s)$ or $He^+(2s)$ ions. Solving the rate equations we find to a good approximation [8] that the F surviving C2 can be written:

$$F=F_0\ \exp\{-[\sigma^{\rm tot}_{\rm de}-(\sigma^{10}_{1s}-\sigma^{10}_{2s})]L_2p_2/kT\}, \qquad (4)$$

where F_0 is the entrant value. The cross sections for electron capture to $He^+(1s)$ and $He^+(2s)$ ions are denoted σ^{10}_{1s} and σ^{10}_{2s}, respectively. L_2 is the effective length [8] of C2, and p_2/nkT gives the Ar number density at room temperature. Combining Eqs. (3) and (4), we get $\sigma^i_{\rm eff}=A^i\exp(-Bp_2)+C^i$, with A^i, B, and C^i given by $A^i=(\sigma^i_{2s}-\sigma^i_{1s})F_0$, $B=[\sigma^{\rm tot}_{\rm de}-(\sigma^{10}_{1s}-\sigma^{10}_{2s})]L_2/kT$, and $C^i=\sigma^i_{1s}$.

Note that B, which represents the total attenuation cross section $\sigma_{\rm att}=\sigma^{\rm tot}_{\rm de}-(\sigma^{10}_{1s}-\sigma^{10}_{2s})$, is independent of F_0 and i (the choice of monitor in C3). Using A^i, B, and C^i as parameters to fit the data in Fig. 3, two independent values for $\sigma_{\rm att}$ were found: $\sigma_{\rm att}({\rm TDI})=(7.35\pm1.01)\times10^{-16}$ cm^2 and $\sigma_{\rm att}({\rm SI})=(7.90\pm1.41)\times10^{-16}$ cm^2, giving a weighted average of $\sigma_{\rm att}=(7.54\pm0.82)\times10^{-16}$ cm^2. Thus since we measure [8] $\sigma^{10}_{1s}-\sigma^{10}_{2s}=(1.0\pm9.2)\times10^{-17}$ cm^2 independently, by comparing the single charge-exchange yields with mixed and ground-state He^+ beams, we obtain the total deexcitation cross section $\sigma^{\rm tot}_{\rm de}=(7.6\pm1.2)\times10^{-16}$ cm^2.

The nonradiative deexcitation cross section $\sigma^{\rm NR}_{\rm de}$ was determined in a separate measurement by varying the pressure of Ar in C3 (C2 now empty) and recording TOF spectra of the kinds shown in Fig. 4.

The $He^+(1s)$ cross sections are $\sigma^{\rm SI}_{1s}=(1.39\pm0.17)\times10^{-17}$ cm^2 and for double ionization (DI) $\sigma^{\rm DI}_{1s}=(2.75\pm1.03)\times10^{-18}$ cm^2, obtained from the spectrum with the field quencher on. By using $F_0=10\%$ we arrive at $\sigma^{\rm SI}_{2s}=(1.94\pm0.46)\times10^{-16}$ cm^2 and $\sigma^{\rm DI}_{2s}=(3.4\pm2.1)\times10^{-17}$ cm^2, which add up to $\sigma^{\rm NR}_{\rm de}=(2.28\pm0.51)\times10^{-16}$ cm^2. Our result for radiative deexcitation thus becomes $\sigma^{\rm R}_{\rm de}=\sigma^{\rm tot}_{\rm de}-\sigma^{\rm NR}_{\rm de}=(5.4\pm1.3)\times10^{-16}$ cm^2 and the branching ratio for radiative deexcitation $R_{\rm BR}=(70\pm8)\%$.

Prior and Wang [6] used a semiclassical, straight-line trajectory approach to derive the rate coefficient for radiative collisional deexcitation by considering the $2s$-$2p$ transitions driven by the induced target dipole field. With a well-defined collision velocity, their result may be represented as a formula for the cross section in atomic units (πa_0^2):

$$\sigma^{\rm R}_{\rm de}=5/3\sqrt{2\alpha_T/(Z_Pv_P)}, \qquad (5)$$

where Z_P is the projectile nuclear charge, α_T is the polarizability of the target, and v_P is the projectile velocity in atomic units [8]. For 6.6-keV $^4He^+$ on Ar, Eq. (5) yields $\sigma^{\rm R}_{\rm de}=9.6\times10^{-16}$ cm^2. Before comparing this to the experimental result, we must correct for the fact that Eq. (5) is derived without taking any competing processes into account. The two most important such processes are electron

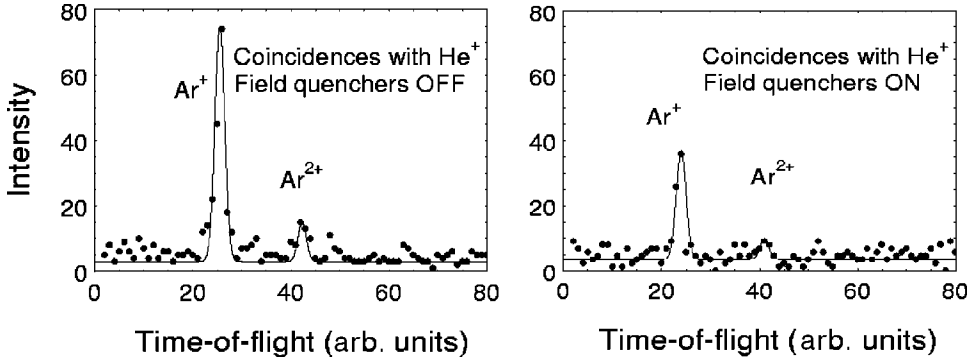

FIG. 4. Time-of-flight spectra showing the pure ionization channels ($He^+ + Ar \rightarrow He^+ + Ar^{q+} + qe^-$, $q=1,2$) for a beam with the initial metastable fraction ($F=F_0$) and for a beam where the metastables have been field quenched ($F=0$). The spectra are recorded for the same ion dose and Xe pressure in C3.

capture to the metastable ion and NR deexcitation, for which we have measured the cross sections [8].

To correct for competing processes, the corresponding transition probability P, as a function of impact parameter b, is in principle needed. In deriving Eq. (5) it is argued [6,8] that for small impact parameters the probability of ending up in the $2p$ state after the collision will oscillate rapidly between zero and unity as a function of b. Within a certain limiting impact parameter, here $b_0 = 3.6a_0$ [8], the average probability is one-half. The probability for the competing mechanisms is expected to be very small for $b > b_0$, due to the lack of the possibility of resonant electron transfer at internuclear distances larger than b_0 [8]. Thus, for a competing process we know that $b < b_0$, and under these conditions a correction can be made without explicit knowledge of $P(b)$. In the absence of the competing processes, the probability for radiative deexcitation would have been one-half in the relevant impact-parameter region. We thus correct for the presence of the competing processes by subtracting half the sum of their measured cross sections. Our resulting semiempirical value is then [8] $\sigma_{\mathrm{de}}^{\mathrm{R}} = 5.3 \times 10^{-16}$ cm^2, which is in agreement with the experimental result $\sigma_{\mathrm{de}}^{R} = (5.4 \pm 1.3) \times 10^{-16}$ cm^2.

In this work we have used a technique to measure separate and absolute cross sections for radiative and nonradiative deexcitation of metastable ions in interactions with atoms. The measured radiative deexcitation cross section for $He^+(2s)$-Ar collisions compares favorably with a semiclassical treatment of $2s$-$2p$ mixing in the field of the induced Ar dipole, provided that competing processes are taken into account. This agreement indicates that the Stark-field mixing mechanism is an appropriate description of the radiative deexcitation mode. Further, we measured the radiative branching ratio to be $(70 \pm 8)\%$. We note that this is similar to the theoretical value for $He^+(2s)$-He collisions at thermal energy [3], which is the only other branching ratio for collisional deexcitation available for comparison. This remarkable coincidence may indicate that the nonradiative deexcitation scales with velocity in a way similar to the radiative part, in spite of the fact that the nonradiative deexcitation mechanisms are expected to be very different for thermal and keV collisions.

Additional experiments encouraged by this pilot experiment include extension to other target atoms and to molecules having permanent electric dipole moments; to smaller v, to explore the changing influence of diabatic molecular curve-crossing mechanisms applicable in the higher v ranges and to probe the slightly lower energy region of principal fusion interest; and to applying our method to find $\sigma_{\mathrm{de}}^{\mathrm{R}}$, $\sigma_{\mathrm{de}}^{\mathrm{NR}}$, and R_{BR} for $H(2s)$ as well as for heavier H-like ions.

This work is supported by the Swedish Natural Science Research Council (Grant Nos. F-GF 08801-315 and F-AA/FU 08801-320), the Danish Natural Science Research Council (Grant No. 9600989), the National Science Foundation (Grant No. PHY-9417924), and by the European Community Commission (Grant No. ERBFMBICT961754).

[1] F. M. Penning, Naturwissenschaften **15**, 818 (1927).

[2] See especially A. Niehaus, Phys. Rep. **186**, 149 (1990); H. Hotop, in *Experimental Methods in the Physical Sciences,* edited by F. B. Dunning and R. G. Hulet, Atomic, Molecular, and Optical Physics: Atoms and Molecules, Vol. 19B (Academic Press, San Diego, 1996), and references therein; P. E. Siska, Rev. Mod. Phys. **65**, 337 (1993).

[3] W. E. Lamb, Jr. and M. S. Skinner, Phys. Rev. **78**, 539 (1950); E. Lipworth and R. Novick, *ibid.* **108**, 1434 (1957); W. E. Lamb, Jr. (private communication).

[4] See material by R. Janev and D. Schultz (Chap. 11) prepared for *Atomic and Molecular Processes in Fusion Edge Plasmas,* edited by R. Janev (Plenum Press, New York, 1995); R. Janev (Atomic and Molecular Data Unit, IAEA, Vienna) (private communciation).

[5] C. A. Kocher, J. E. Clendenin, and R. Novick, Phys. Rev. Lett. **29**, 615 (1972).

[6] M. H. Prior and E. C. Wang, Phys. Rev. A **9**, 2383 (1974).

[7] M. B. Shah and H. B. Gilbody, J. Phys. B **9**, 2685 (1976); **9**, 1933 (1976).

[8] H. T. Schmidt, S. H. Schwartz, A. Fardi, K. Haghighat, H. Cederquist, L. Liljeby, A. Langereis, J. C. Levin, and I. A. Sellin (unpublished).